

Research article

Weather effects on pollution and acid rain on the Mediterranean slope of the Iberian System

J. Quereda Sala¹, E. Montón Chiva, V. Quereda Vázquez and B. Mollá Cantavella

¹Laboratory of Climate, University Jaume I
E-mail address: quereda@his.uji.es
Fax: +34 964 729265
Tel.: +34 729962



This work is licensed under a [Creative Commons Attribution 4.0 International License](http://creativecommons.org/licenses/by/4.0/).

ABSTRACT

Knowledge of atmospheric scenarios constitutes one of the essentials of environmental analysis. These scenarios will adopt particular significance in a region with very complex topography and orographic effects, such as found on the Mediterranean slope of the Iberian System. This region is characterized by the dominance of localized atmospheric stability. It is further complicated by the installation of a 1.05 GW ENDESA thermal power plant in Teruel, Andorra during 1979 and 1980. The main fuel of the energy plant consists of the lignite and bituminous coal of Andorra's town and surrounding areas, having a high sulphur content of 7%.

The numerical implementation of Gaussian dispersion models (Briggs and Holland) has been validated through immission data recorded by the Valencian Community Atmospheric Monitoring Network (at Coratxar and Morella), and permits the identification of fluctuations in the immission values of SO₂ and recorded pH. Simultaneously it has been possible to identify that these fluctuations are explained by the different weather conditions within which these have arisen. This has allowed the identification of characteristic weather conditions, with respect to pollution and acid rain, as being a key factor in models for environmental management.

Keywords: atmospheric scenarios, environmental analysis, acid rain, Gaussian dispersion models, geographic layer, air pollution, air quality, transportation meteorology.

1. INTRODUCTION AND IMPORTANCE

Knowledge of atmospheric scenarios constitutes one of the essentials of environmental analysis. Every statement regarding the quality of air and water will be open to severe errors if a rigorous determination of atmospheric conditions is not performed. There is little wonder over this when it is precisely this environment where atmospheric pollutants are injected, transformed, disseminated and precipitated. These processes are especially

noticeable with acid rain, occurring when SO_2 and NO_x emissions interact in the atmosphere with water, oxygen and other chemicals to form acidic compounds. These compounds pass from the atmosphere to the soil and, as a consequence, can explain the phytotoxic damage that has been observed in certain forest masses (Montalvo et al, 1993; ICONA, 1991; Johnson and Sicama, 1983).

These scenarios will adopt particular significance in a region with very complex topography and orographic effects, such as found on the Mediterranean slope of the Iberian System. It is further complicated by the installation of a 1.05 GW ENDESA thermal power plant in Teruel, Andorra, during 1979 and 1980 (Fig. 1). The main fuel of the energy plant consists of the lignite and bituminous coal of Andorra's town and surrounding areas, having a sulphur content of 7%. Currently the Wet Flue desulphurization process, installed since 2000, manages to remove over 90% of the SO_2 content.

The installation of the Wet Flue desulphurization plant posed an important technological challenge given the design requirements necessary to deal with the high sulphur content of the local fuel. The immense volume of gases produced during combustion, as well as the high concentration of sulphur, made the design one of the largest in the world both in terms of capacity and specific retention. This technical difficulty and the lack of suitable prior references have required both the plant itself, as well as the process, to be optimised over the years.

One of the principal problems faced during the initial years of operation was the need for frequent stops due to either group breakdowns and blockages, or simple cleaning activities. The shutdown of one or more of these desulphurization groups during days or even months created a significant decline in the efficiency of the plant.

In 2007, motivated in part by the Kyoto protocol, the three absorbers in the design were refurbished and the efficiency of the plant was greatly improved by the installation of a seventh pump in the recirculation system, a doubling of the number of sprays and a more constant replacement of the "clean" slurry. In addition, the works included coating the inner walls of the absorbers with Hastelloy, a nickel alloy highly resistant to corrosion caused by sulphur, as well as the replacement of the entire recirculation system and other details common to the three buildings housing the desulphurization plant. In this way ENDESA managed to prolong the life of the whole mechanism, reducing the number of stoppages and speeding up the cleaning of equipment. As can be seen in the graph (Fig. 2) the refurbishment achieved optimal results in terms of improving the efficiency of the desulphurization plant from 2008 onwards, dramatically reducing specific SO_2 emissions to the atmosphere to below 90% of the risk threshold.

2. THE PREDOMINANT STABILITY OF THE GEOGRAPHIC LAYER OF THE ATMOSPHERE ALONG THE MEDITERRANEAN COASTLINE: A VERTICAL THERMAL STRUCTURE FAVOURABLE TO THE DISCHARGE OF POLLUTANTS.

Compared to the neutral or unstable conditions prevalent in a large part of temperate zone countries (Millán and Sanz, 1992), the Mediterranean coastal region is characterised by the dominance of atmospheric stability. This stability, more or less absolute, corresponds to a weather system with stable stratification and a lack of, or distinct limitation to, upward movements in the atmosphere. In this way particles and pollutants appear constrained and more or less stratified in the geographic (friction) layer. This lowest layer of the troposphere contains a fluid that has been in recent contact with the Earth's surface and that has been transferred to the upper layers by turbulent diffusion, usually in less than one day (San José et al, 1984).

The greatest difficulty in defining this geographical or friction layer lies in determining its upper limit. The limit is without doubt the first thermal inversion layer over the region. However, it is a variable limit because the inversion layer presents frequent fluctuations in height according to weather and season. Regional analysis shows that it is often present at pressures between 820 and 880 millibars, that is at altitudes of 1.3 to 1.5 km. Similarly, the average state curve shows, especially in winter, the existence of a regional low inversion layer at 950 hPa (0.5 km) (Fig. 3).

Under these conditions the convection of any contaminant is arrested by these inversion layers, which act as a cover hindering external dissemination (Fig. 4).

In the case of a stable atmosphere, which is the most frequent structure in the region, the thermal and dynamic draw of the chimney plume (ΔH) is given by Briggs' formula (Hanna et al, 1982):

$$\Delta H = 2.6 \left(\frac{F}{U_{ch} \cdot S} \right)^{1/3} \quad (1)$$

Where:

$$F = g \cdot v_s \cdot \frac{D^2}{4} \cdot \frac{T_s - T_a}{T_s} \quad (2)$$

$$S = \left(\frac{g}{T_a} \right) \cdot \left(0.01 + \frac{\Delta T}{\Delta z} \right) \quad (3)$$

Under the average atmospheric and regional parameters, output speed of the gases (V_s), diameter of the chimney (D) and outlet temperatures of gas (T_s) and ambient air (T_a), the plume rise around the area of the thermal power plant reaches heights of 300 to 400 metres. This means that the dispersion of the plume could ascend to the height of the first regional inversion layer placed at 875-850 hPa. Hence the emitted pollutants only affect the environment under atmospheric conditions where the plume rise isn't able to exceed this layer. The fluctuation of immission values in this regional environment, within the framework of stability, therefore appears closely linked to the thickness of the atmospheric mixing layer and the turbulence (wind speed). This provides a key component to the general term Gaussian dispersion model:

$$C(x, y, z, H_e) = \frac{G}{2\pi\sigma_y \sigma_z u_{ch}} \exp\left(-\frac{y^2}{2\sigma_y^2}\right) \left\{ \exp\left(-\frac{(H_e - z)^2}{2\sigma_z^2}\right) + \exp\left(-\frac{(H_e + z)^2}{2\sigma_z^2}\right) \right\} \quad (4)$$

Where:

C = Concentration of the chemical in the air.

G = Rate of chemical emission.

U_{ch} = Wind speed in horizontal direction at chimney height.

H_e = Effective chimney stack height.

y = Horizontal distance from plume centerline.

z = Vertical distance from the ground level.

σ_y and σ_z = Components of lateral and vertical wind dispersion, dependent on turbulence and the thickness of the mixing layer.

The Maximum Ground Level Concentration (MGLC) is usually of interest. It will occur at some downwind distance right below the centerline of the plume ($y=0, z=0$) then Eq. 4 is reduced to:

$$C(x, 0, 0, H_e) = \frac{G}{\pi\sigma_y \sigma_z u_{ch}} \exp\left(-\frac{H_e^2}{2\sigma_z^2}\right) \quad (5)$$

Where it is necessary to calculate the coefficients σ_y and σ_z , for lateral and vertical wind dispersion, the following can be used (Puigcerver and Carrascal, 2008: 150):

$$\sigma_{y,z} = m \cdot x \cdot (1 + n \cdot x)^p \quad (6)$$

Where variable coefficients and exponents are according to the Pasquill-Gifford stability classes.

The numerical implementation of Gaussian dispersion models (Briggs and Holland), using the Industrial Source Complex (ISC) model developed by the US Environmental Protection Agency (EPA), has been validated through immission data recorded by the Valencian Community Atmospheric Monitoring Network (at Coratxar and Morella). To highlight this, the data for the maximum hourly peak, recorded during January 13th 2012 at 254 $\mu\text{g}/\text{m}^3$ in Coratxar, corresponds to the Gaussian models of Briggs and Holland (Figs. 5 and 6).

The same application, for the atmospheric profile on January 6th, 2012 (Figs. 7 and 8), with a mixing layer greater than 600 metres and a wind speed of 12 m/s, provides a theoretical value of SO_2 immission of only 1-2 $\mu\text{g}/\text{m}^3$, identical to that recorded at the stations of Coratxar and Torre Miró (Valencian Community Atmospheric Monitoring Network). Both stations are located along the axis of the prevailing air flows.

3. WEATHER CONDITIONS AND ACID RAIN

Within the framework of these structures related to atmospheric stability, the precipitation of acidic pollutants has been linked, by nature of the process, to situations of conditional stability. Between 2005 and 2012 these processes have been studied by an automatic rainwater pH analyser (Kimoto, AR-106) (Fig. 9), annually calibrated and controlled through ad hoc measures both in the field and in the laboratory.

The overall evolution of the rainwater pH in the Maestrazgo region (Morella) between 2005 and 2012, along with pluviometric records, is represented in figure 10. The curve shows the fluctuations of the pH with respect to the average threshold of acidity, 5.5. The recording was carried out by taking averages every ten minutes for all rainfall lasting an hour or more (greater than 6 records). In total more 1100 measurements were obtained in this way over the period. The results have given an average pH of 5.67 in Torre Miró (Morella). This value allows us to consider that the average pH of rainwater has remained unchanged from the eighties (AMBIO, 1992; Carratalá, 1992). The measured values of pH in rainwater in the sparse studies performed are, for the most part, greater than 5.4, so in general we cannot talk about "acid rain". However, these same studies show that there are some stations which have registered pH values lower than 5.0 relatively frequently (Torre Miró, Fredes). This has in the past been explained by the decrease of the marine contributions of sodium and magnesium ions as well as the biogeographic variation in these inland and mountainous areas, diminishing the neutralizing effect on the acidity. Hence the lower pH values recorded in the inland and mountainous areas and perhaps in the northernmost parts of the Valencian Community.

This explanation of acidifying processes cannot be sustained in light of our research on rainfall records for these years (2005-2012). The average pH value in rainwater, 5.67, and conductivity values do not seem to correspond to the serious changes of acidification that have been made and that would be expected in the surrounding region of the thermal power plant. However, the obtained series show episodes of strong acidification versus others of basic or alkaline nature. These fluctuations are explained by the different weather conditions in which they were produced.

3.1. Conditions for strong acidification

In the order of scenarios, the most characteristic atmospheric condition for these acid rains ($\text{pH} < 5.5$) has been associated mainly with the convergence of two factors. The first is the existence of an inversion layer located between 2.0 and 2.5 km over the limit of the gas plume of the thermal power plant that traps the emission of pollutants. The second factor is the influx of winds over the Maestrazgo and Els Ports that carry the emitted pollutants. This advection factor is further amplified when, in addition to local pollutants, a cross-border transport of high-intensity emissions of generated pollutants occurs from the largest Mediterranean power plants in Italy and France (Piombino and Fos Berre).

An example of the most severe cases, with recorded values of pH around 4.5 (Fig. 11), is the situation corresponding to the first days of January 2006. The constant NE / NNE winds provided the cross-border pollutants in the area (Fig. 12). These pollutants were trapped under the inversion layer located at 2000 metres (Fig. 13).

Typically, all the records of significant acid rain have corresponded to this situation of conditioned atmospheric stability with an inversion layer located between 2 and 3 km. The atmospheric conditions on the 13th February 2008 are quite expressive (Fig. 14). This situation represents the time of highest acidification since 2005 (Fig. 15). The reported general inversion at 725-700 hPa is ventilated by steady winds at about 850 hPa. These winds were the advection of the large emissions of air pollution from the thermal power plants in Italy and France, in addition to Andorra's thermal power plant. This cross-border flow, together with the local contribution, helped once again to intensify the acidification processes over the Maestrazgo (Fig. 16).

The same burst of cold air, a proponent of polluting emissions, also determined the thermohygroscopic conditions favourable to acid precipitation. The dewpoint temperature (T_d) remained above the average air

temperature during the 13th to 15th February. A persistent fog covered the tops of the Maestrazgo and in its interior acidifying reactions occurred (Fig. 17).

3.2. Conditions for acid rain neutralization

They are produced under atmospheric conditions in which the air advection involves the extension of African aerosols at the regional level. Consequently we must emphasize that the regional average pH value, 6.67, could be considerably lower if we did not take into account a factor of great importance in the masking or neutralization of acid rain. This factor is the constant presence, especially in summer, of aerosols of African origin covering much of the Western Mediterranean. These aerosols are, together with the basic nature of the local ecosystem, responsible for the peaks of pH greater than 6. The chemical analysis of major times of mud rain has yielded the following results (Quereda et al, 1996): pH: 7.86; calcium: 21.20 ppm; magnesium: 0.60 ppm; sodium: 3.30 ppm; potassium: 6.10 ppm.

The best indicator of these atmospheric processes is displayed by one of the latest episodes that we have recorded. The first corresponds to the development from the 19th to 24th May 2007. The atmospheric conditions determining the rainfall was a “cold drop” (cut-off low) on the vertical plane of the Gulf of Cadiz (Fig. 18) pressing on the mass of subtropical continental air.

The pH values recorded at the beginning of this episode reach a peak of pH = 7 (Fig. 19). The beginning of the precipitation is when the mud rain is most intense. As the precipitation continues, the atmosphere is washed and the pH returns to normal values of 5.5 – 6.0. All these phenomena occur under atmospheric conditions that already anticipate the summer model with an accompanying persistence of this coverage of African dust (Fig. 20).

In a paradigmatic way, these conditions return to characterize the period of intense rain showers that defined the last week of August 2012 (Fig. 21). The atmospheric structure shows the emergence of a powerful African aerosol that has extended from the north of Africa to the whole western Mediterranean basin (Fig. 22).

4. CONCLUSIONS

The territory of Maestrazgo and the Els Ports Nature Reserve of Tortosa, located in the Mediterranean slope of the Iberian System, are continuously experiencing a circulatory flow from the west that transports the emissions of pollutants from the thermal power plant at Andorra (Teruel). These emissions, together with the detection of phytotoxic effects in the forest masses of the area have instigated a high level of monitoring on air quality, as well as the installation of efficient FGD systems (Flue Gas Desulphurization).

This efficiency of the current system of desulphurization (Mitsubishi) at the Andorra plant, together with regulating local area emissions, are why the impact of environmental pollution is kept below the risk thresholds established in current regulations on emission control. Simultaneously it has been possible to identify that the fluctuations in the immission values of SO₂ and recorded pH are explained by the different weather conditions within which these have arisen. This has allowed the identification of characteristic weather conditions, with respect to pollution and acid rain, as being a key factor in models for environmental management.

The conditions that favour an increase in the effect of pollutant emissions which are present in the area, are where they are constrained in the lower levels by a regional inversion layer located at 850 hPa. This is an inversion layer that produces a mixing layer which is less thick and turbulent. This acidifier situation becomes pronounced with the advection of air flows that, under the inversion layer, transport the emissions of the large thermal plants of the Italian and French Mediterranean. On the other hand, if the air advection is also governed by the African aerosol, the acidity is neutralized and the pH becomes alkaline.

REFERENCES

- [1] AMBIO, S. A. (1992): *Análisis de los valores obtenidos en la red de inmisión del Maestrazgo desde su puesta en marcha (1984-1991)*, Memoria ENDESA, 58 pp.
- [2] BARRENO, E. & FOS, S. (1998): *Seguimiento de la calidad atmosférica en las comarcas de Els Ports y Maestrazgo mediante bioindicadores vegetales (Briófitos y líquenes)*. Informe final, 1994-1997. Empresa Nacional de Electricidad S. A. (ENDESA).

- [3] BRIGGS, G.A. (1975): "Plume rise predictions", Lectures on air pollution and environmental impact analysis. *American Meteorological Society*, Boston, U.S. pp. 59-111.
- [4] CARRATALÁ, A., BELLOT, J., LLEDÓ, M. J. & Gómez, A. (1992): "Composición química del agua de lluvia en la Comunidad Valenciana: resultados preliminares de una red para el control de la calidad ambiental". *Tecnología del Agua*, XII, 101, pp. 17-23.
- [5] CARSON, E. J. & MOSES, H. (1969): "The Validity of Several Plume Rise Formulas", *Journal of the Air Pollution Control Association*, 19:11, pp. 862-866. <http://eur-lex.europa.eu/>
- [6] COUNCIL DIRECTIVE 96/62/CE of 27 September 1996 on ambient air quality assessment and management. *Official Journal L 296*, 21/11/1996, p. 55-63. <http://eur-lex.europa.eu/>
- [7] COUNCIL DIRECTIVE 1999/30/EC of 22 April 1999 relating to limit values for sulphur dioxide, nitrogen dioxide and oxides of nitrogen, particulate matter and lead in ambient air. *Official Journal L 163*, 29/6/1999, p. 41-60.
- [8] Data Summary of 1985 SF Tracer Experiments at Andorra Power Plan. Final Report (NILU). Sep. 1985.
- [9] HANNA, S. R., BRIGGS, G.A. and HOSKER, R. P. (1982): *Handbook on Atmospheric Diffusion*. DOE/TIC-11223, Department of Energy, 102 pp.
- [10] I.C.O.N.A. (1988): "Resumen de las defoliaciones de los puntos de Castellón". ICONA (Instituto para la Conservación de la Naturaleza), Ministerio de Agricultura, Pesca y Alimentación.
- [11] I.C.O.N.A. (1991): "Información diversa de I.C.O.N.A. sobre la situación de las masas forestales de la Comarca de Els Ports (Castellón)". ICONA (Instituto para la Conservación de la Naturaleza), Ministerio de Agricultura, Pesca y Alimentación.
- [12] JOHNSON, A. H. & SICAMA, T. G. (1983): "Acid deposition and forest decline". *Environmental Science and Technology*, 17, pp. 294-305, A.
- [13] KOMIN, G.E. (1981): "Ecological Essence of Forest Cyclic Dynamics". *Ecologiya* 3, pp. 46-53.
- [14] MCMILLIN, C.W. (1982): "Application of Automatic Image Analysis to Wood Science". *Wood Science* 14 (3), pp. 97-115.
- [15] MÉGIE, G. (1996): "Ozone et propriétés oxydantes de la troposphère". *La Météorologie*, 8, 13, pp. 11-28.
- [16] MILLAN, M., ARTIÑANO, B. and ALONSO, L. (1992): *Mesometeorological Cycles of Air Pollution in the Iberian Peninsula*. Commission of the European Communities. Directorate General for Science, Research and Development. Environment Research Programme, 219 pp.
- [17] MILLAN, M & SANZ, M. J. (1993): *La contaminación atmosférica en la Comunidad Valenciana*. Informes CEAM, 93, I, 151 pp.
- [18] MONTALVO, J., QUEREDA, J., BARRENO, E., SERENA, J. M., DÍAZ-PINEDA, F., ROBREDO, F., BERROCAL, M., COSTA, M., SÁNCHEZ, J., LAPEÑA, L., HERNÁNDEZ, F. & ANTOLÍN, C. (1993): *Dictamen sobre la información aportada y conclusiones obtenidas por los estudios realizados sobre la incidencia ambiental de la Central Térmica de E.N.D.E.S.A. en Andorra (Teruel)*. Informe técnico, Universitat Jaume I. 60 pp.
- [19] PUIGSERVER, M. & CARRASCAL, M. D. (2008): *El medio atmosférico: meteorología y contaminación*. Publicacions i edicions Universitat de Barcelona, 248 pp.
- [20] QUEREDA, J., OLCINA, J. & MONTON, E. (1996): "Red dust Rains within the Spanish Mediterranean Area". *Climatic Change*, 32, pp. 215-228, U. S.

[21] REAL DECRETO 1073/2002 de 18 de octubre, sobre evaluación y gestión de la calidad del aire ambiente en relación con el dióxido de azufre, dióxido de nitrógeno, óxidos de nitrógeno, partículas, plomo, benceno, y monóxido de carbono. Boletín Oficial del Estado, nº 260, 30/10/2002, pp. 38020-38033. <http://www.boe.es>

[22] REAL DECRETO 1796/2003 de 26 de diciembre, relativo al ozono en el aire ambiente. Boletín Oficial del Estado, nº 11, 13/1/2004, pp. 1071-1081. <http://www.boe.es>

[23] RED VALENCIANA de Vigilancia de la Contaminación atmosférica (GV). <http://www.cma.gva.es>

[24] SAN JOSÉ, R., CASANOVA, J. L., VILORIA, R. E. y CASANOVA, J. (1984): *Torres meteorológicas y determinación de parámetros turbulentos*, Universidad de Valladolid, 87 pp.

[25] Technology Transfer Network Support Center for Regulatory Atmospheric Modeling. http://www.epa.gov/scram001/dispersion_alt.htm

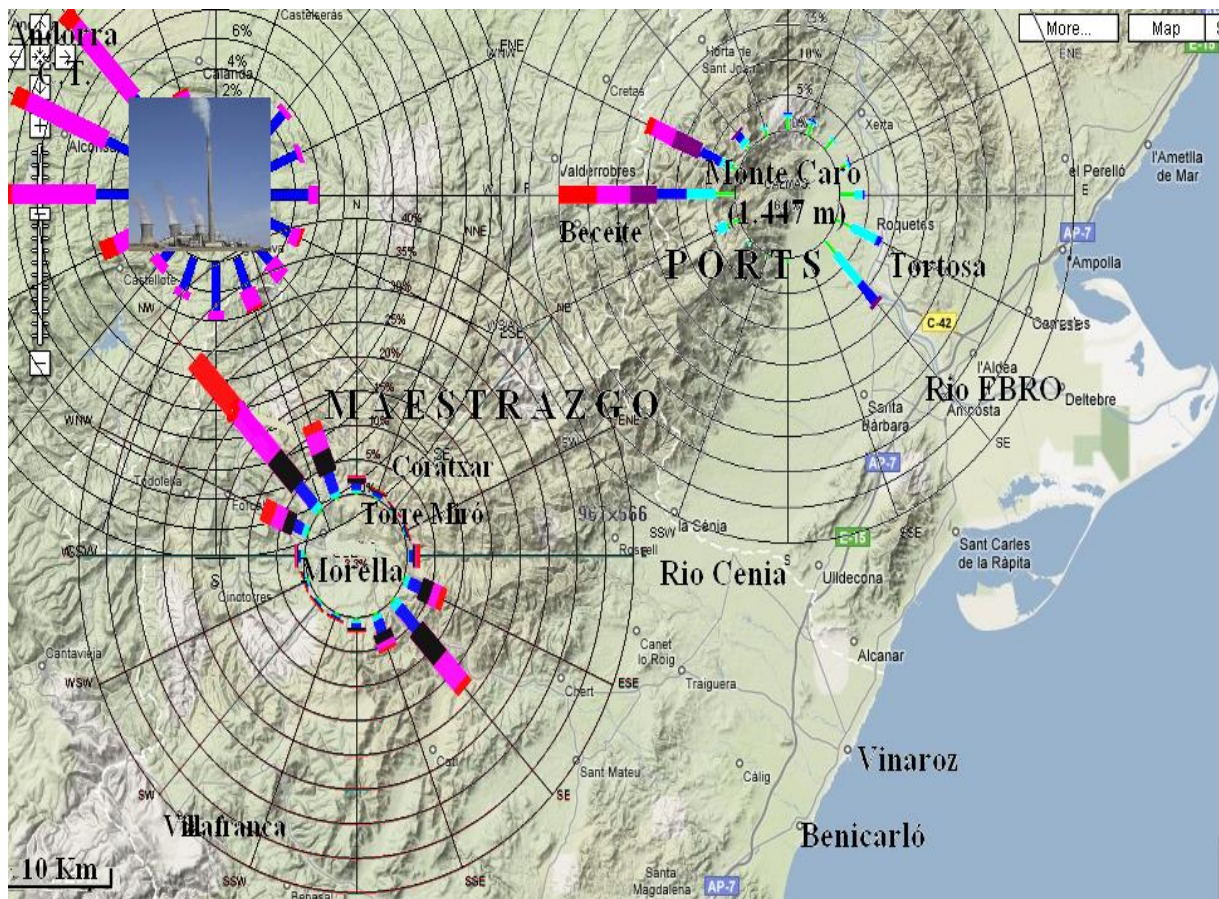


Figure 1: Region of analysis, covering the Maestrazgo and Els Ports Nature Reserve, showing the wind roses of Mount Caro, 1447 m, Torre Miró (1259 m) (Meteorological Network of Jaume I University) and the ENDESA thermal plant of Andorra (685 m). The wind rose of mount Caro is specific in its location, occupying the most frequent height of the inversion layer over which the wind is geostrophic.

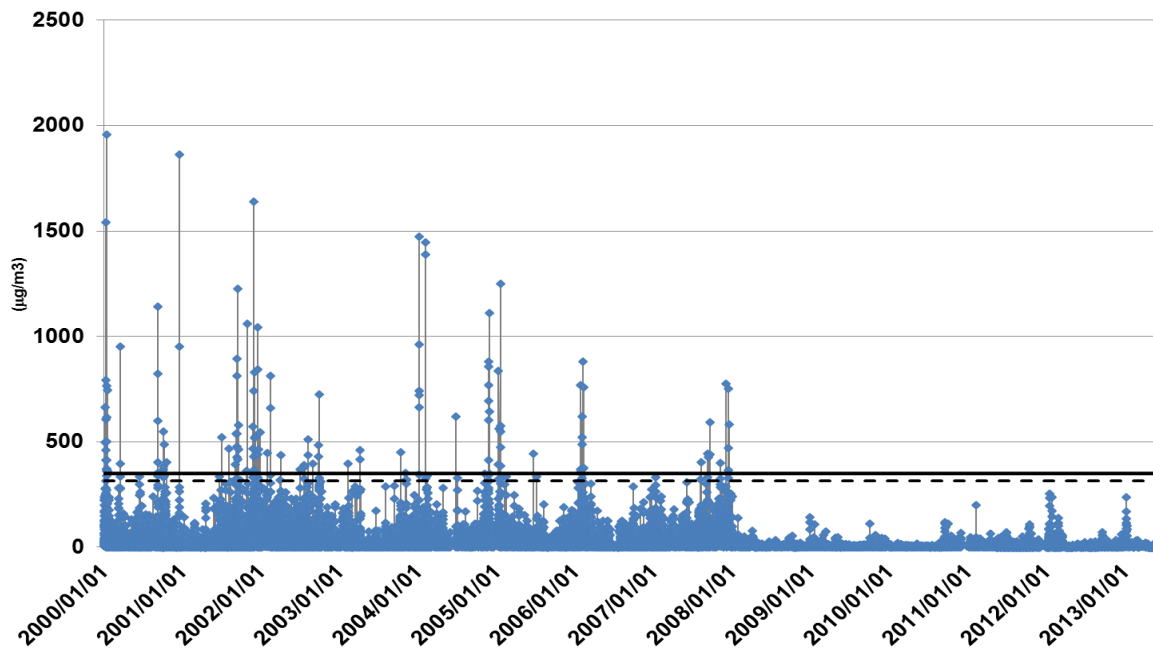


Figure 2: Hourly data of SO₂ immissions ($\mu\text{g}/\text{m}^3$) at Coratxar (Tinença de Benifassà), (Valencian community network for atmospheric monitoring, 2000-2013). The solid and dashed lines represent 100% and 90% of the risk threshold respectively. (Council Directive 96/62/EC, Council Directive 1999/30/EC, Real Decreto 1073/2002 and Real Decreto 1796/2003.)

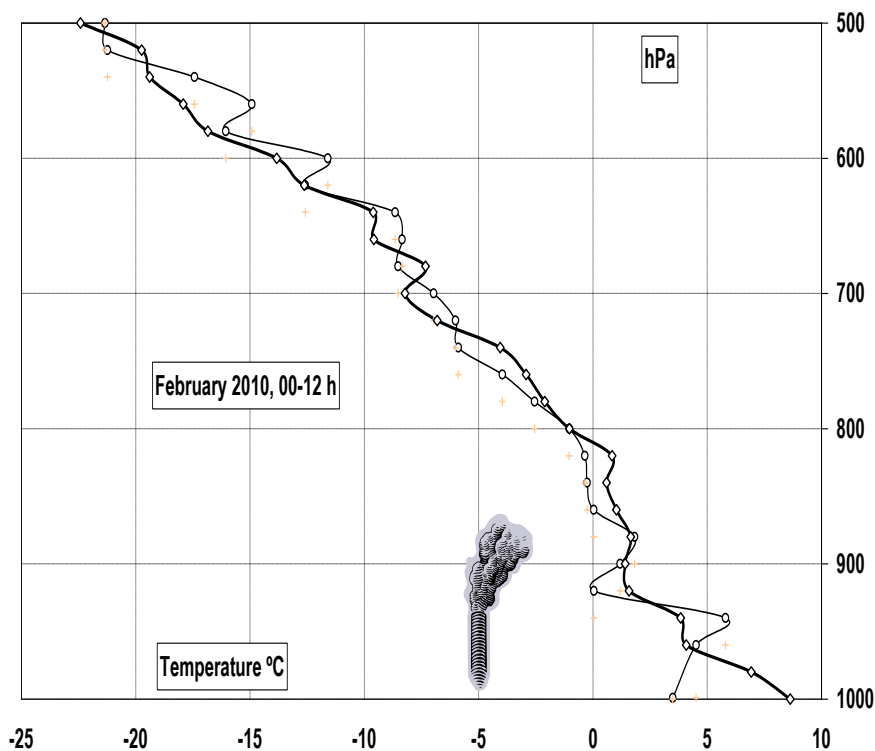


Figure 3: Radiosonde data, Zaragoza airport (AEMET), located 60 km from ENDESA thermal power plant of Andorra. The inversion layer is significantly noticeable at 820-880 hPa



Figure 4: Inversion layer over the Tortosa-Beseit Nature Reserve. Picture taken from the top of Mount Caro (1447 m).

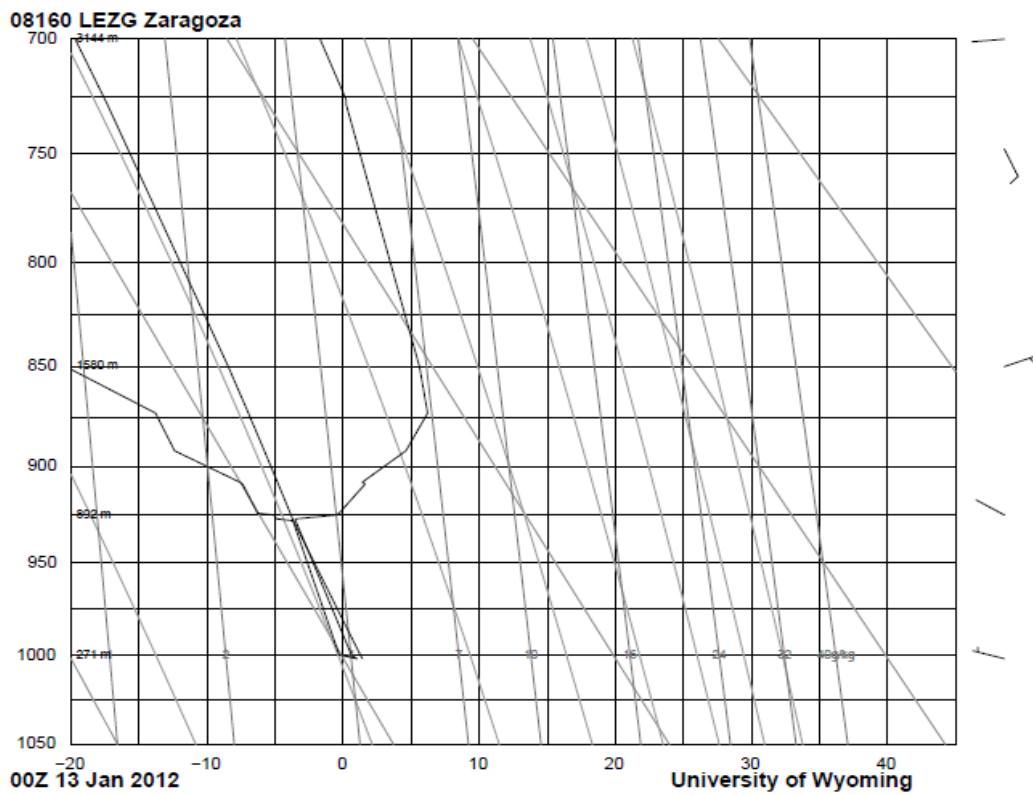


Figure 5: Radiosonde data, Zaragoza, on January 13th, 2012, at 00 hours. Remarkable inversion layer between 925 and 875 hPa, thickness of the mixing layer: 450 metres, and with calm wind < 1m/s.

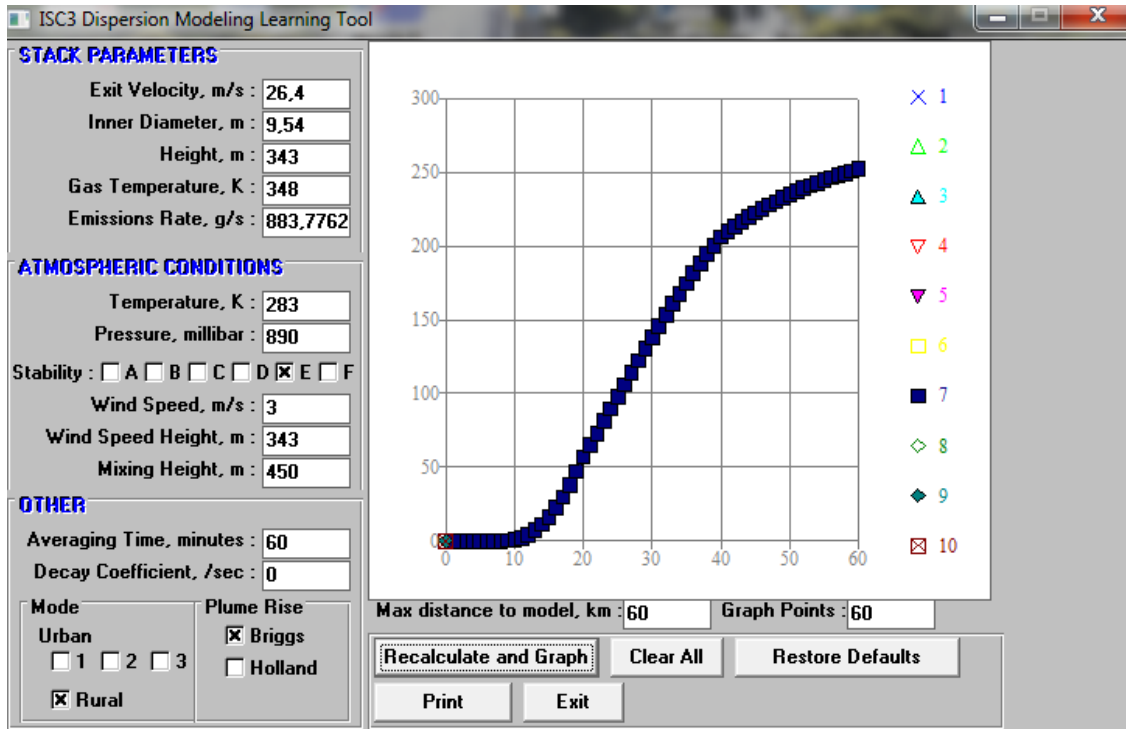


Figure 6: Spread of the plume and SO₂ concentrations between the thermal power plant and a horizon of 60 km (January 13th, 2012).

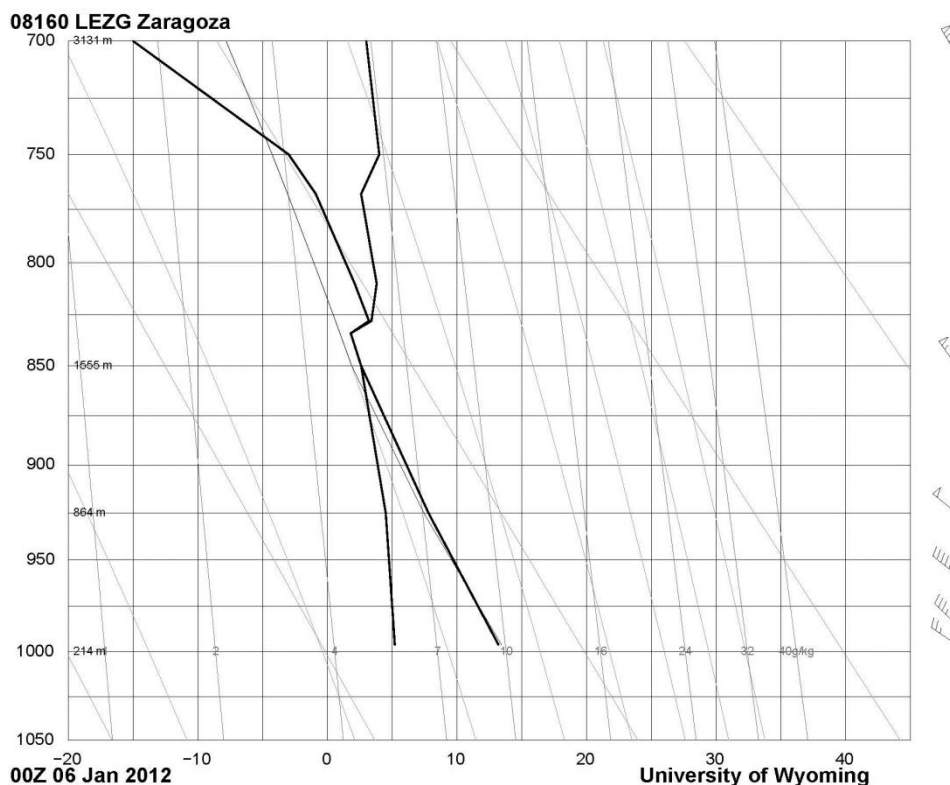


Figure 7: Radiosonde data, Zaragoza, on January 6th, 2012, at 00 hours. The inversion layer appears very high (825 hPa), with strong winds around 12 m/s and a mixing layer > 600 metres.

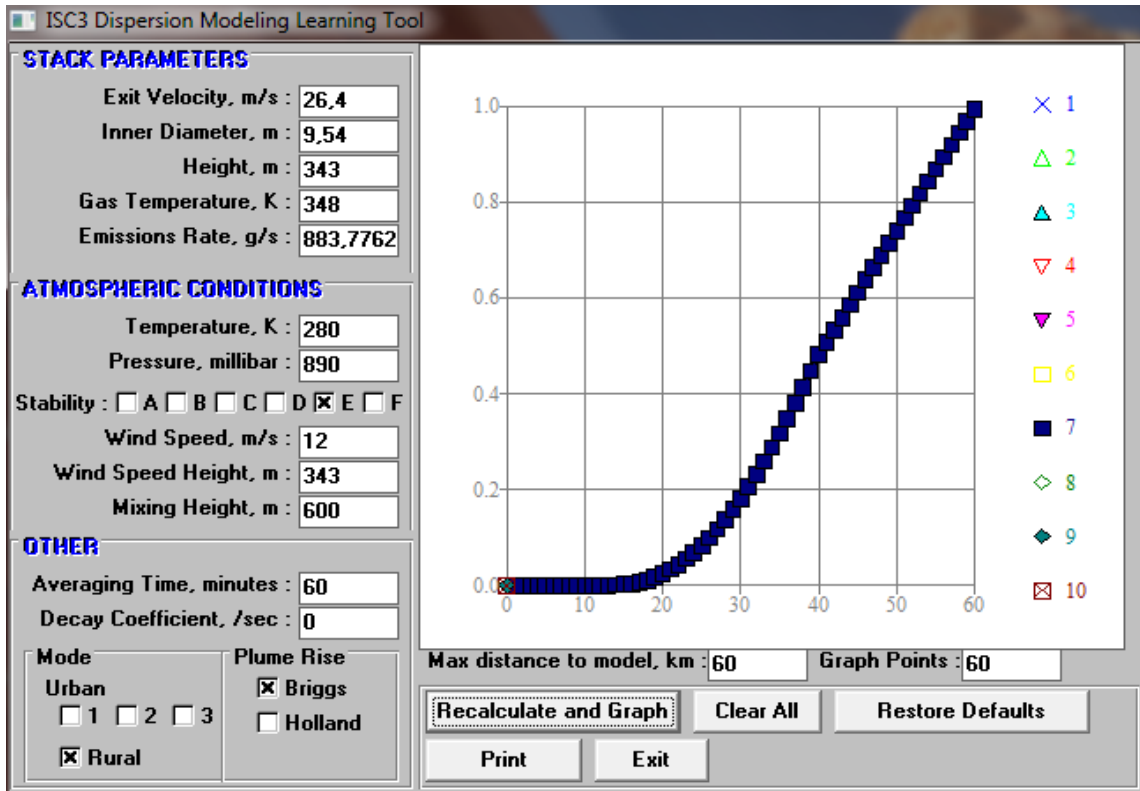


Figure 8: Spread of the plume and SO₂ concentrations between the thermal power plant and a horizon of 60 km (January 6th, 2012).



Figure 9: Kimoto AR-106 acid rain analyser installed at Torre Miró (1223 m).

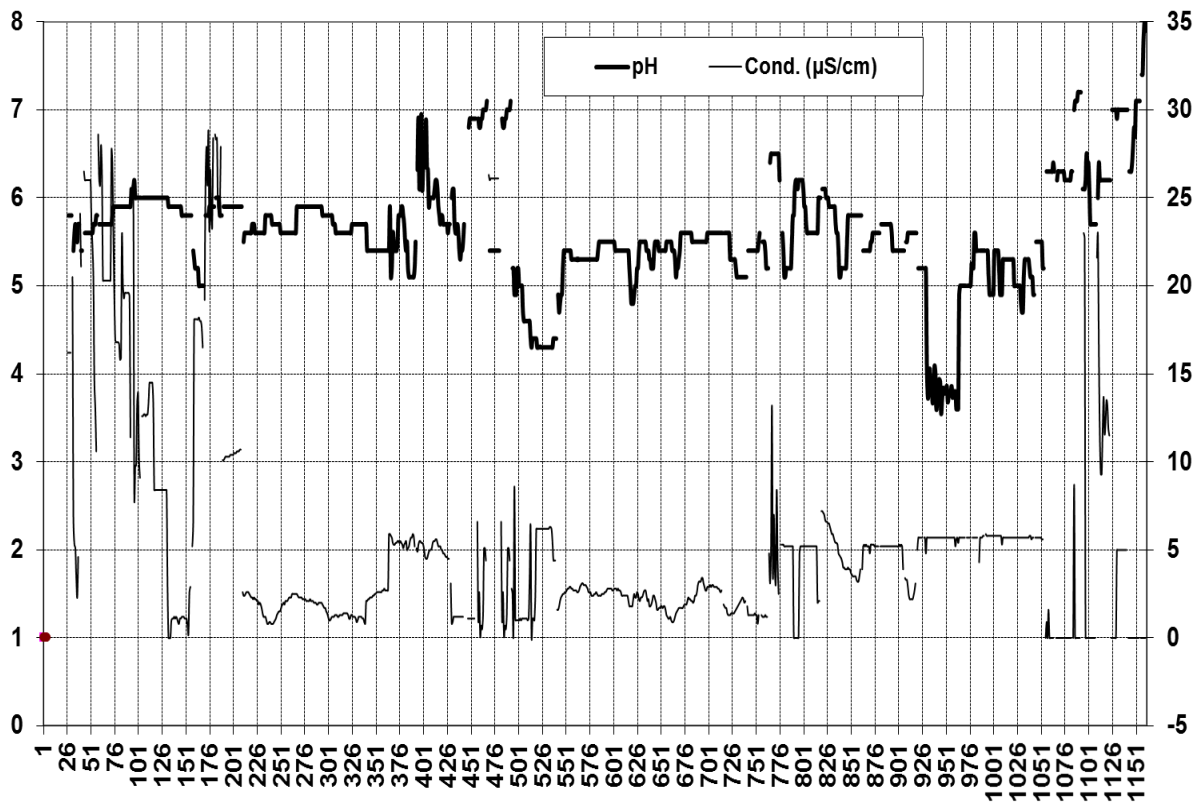


Figure 10: pH value and conductivity in rain water in Torre Miró, Morella (2005-2012). The values correspond to averages every ten minutes in each episode of rain with more than 6 records.

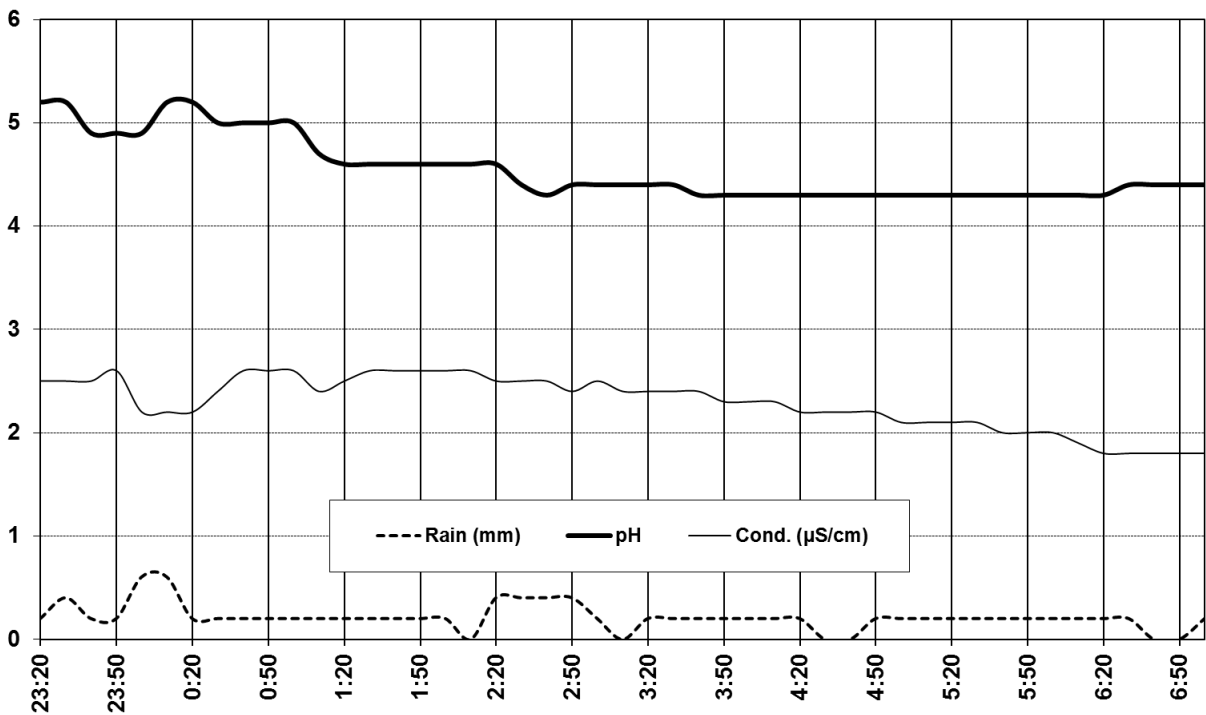


Figure 11: Analysis of rainwater precipitated during the 4th and 5th of January 2006.

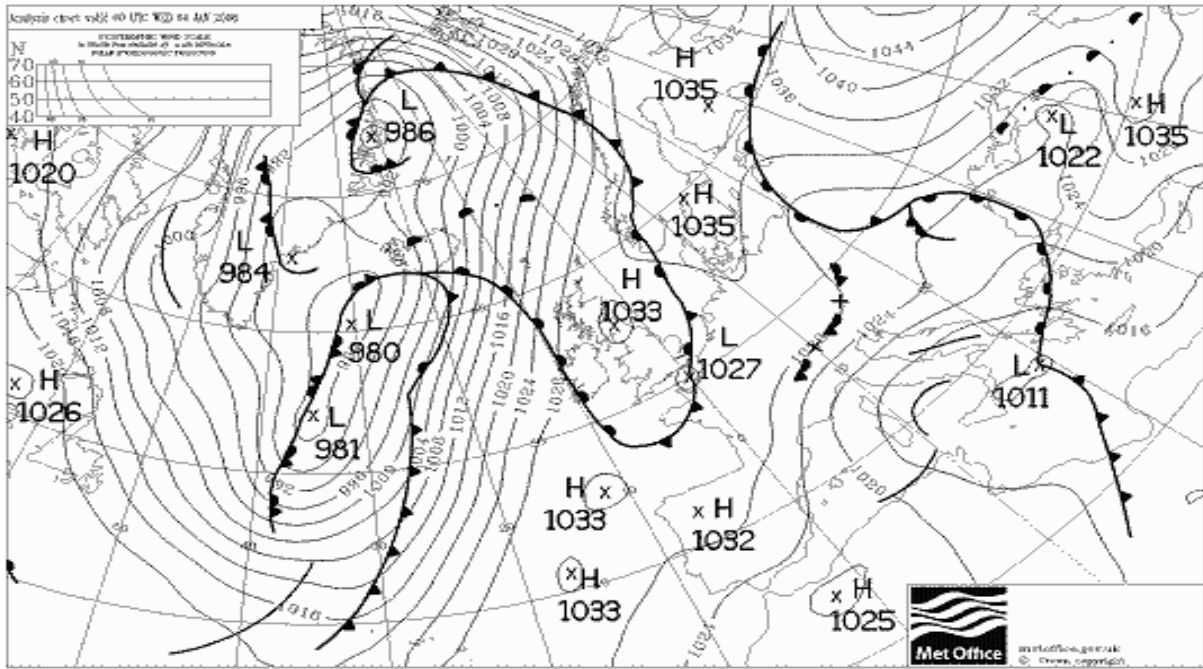


Figure 12: Surface chart, January 4th, 2006. A marked depression over the central Mediterranean sends winds toward the Spanish Mediterranean region. The powerful continental anticyclone channels NE winds that bring the emissions of the thermal power plants that skirt the Alpine arc between Piombino and Andorra's own thermal power plant.

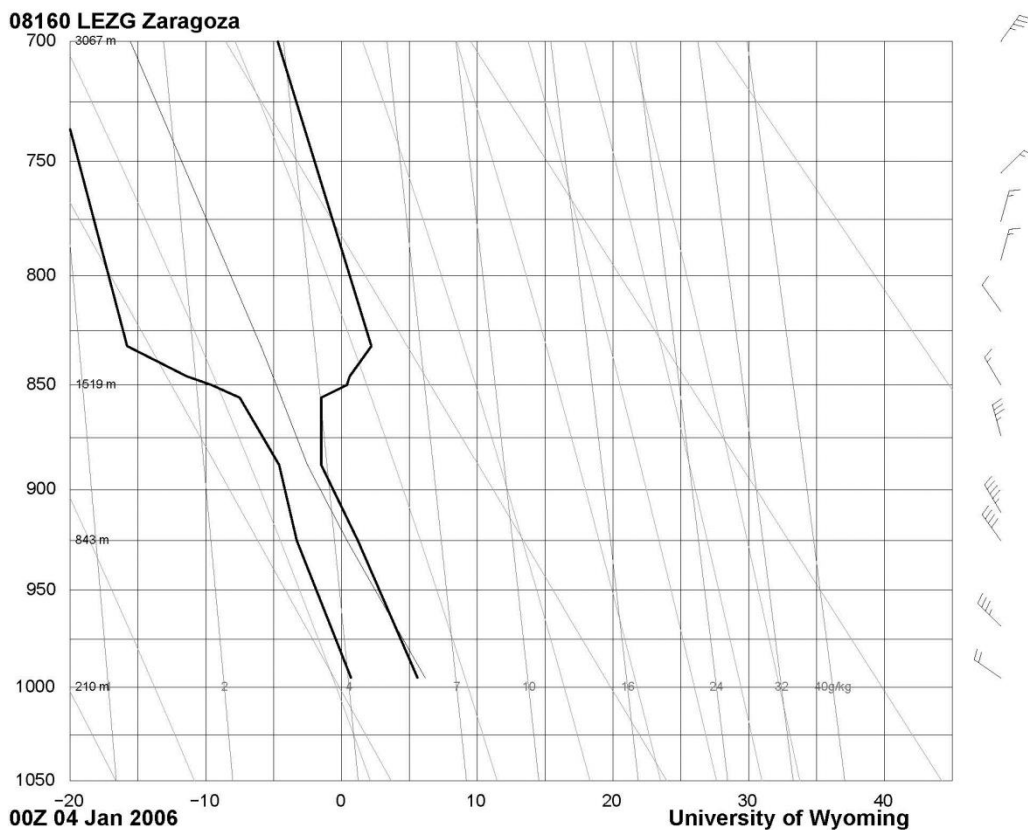


Figure 13: Radiosonde data, Zaragoza, on January 4th, 2006, at 00 hours. The conditional stability in the geographical layer joins a temperature inversion at 2000 m.

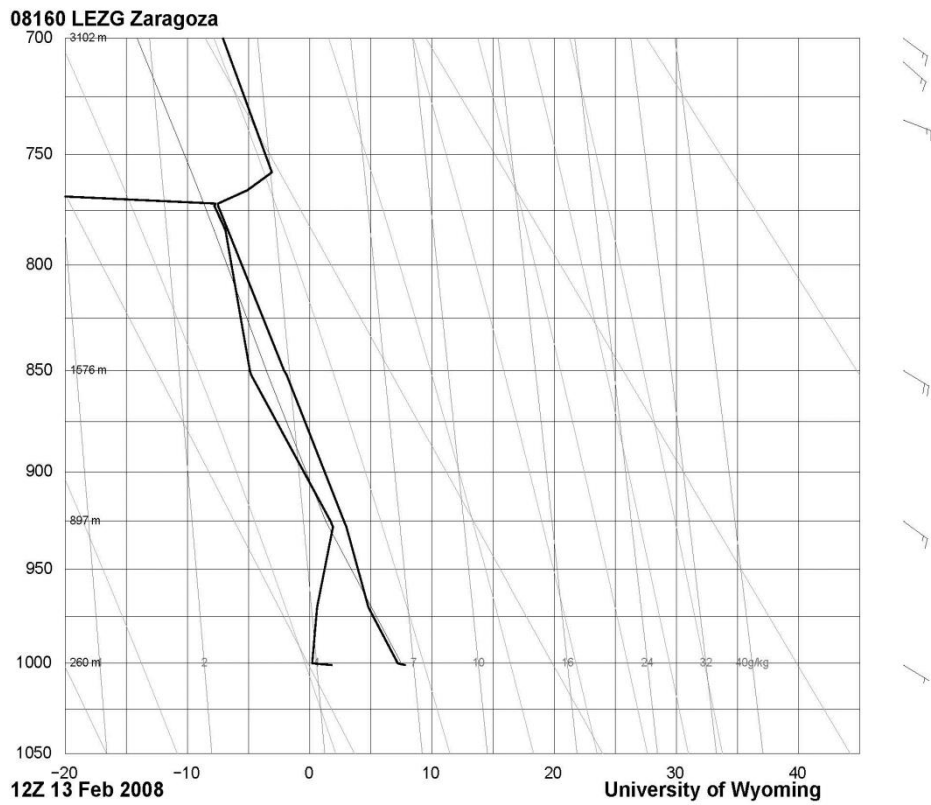


Figure 14: Radiosonde data, Zaragoza, on February 13th, 2008 at 00 hours. Conditional stability in the geographical layer joins a temperature inversion at 3000 m.

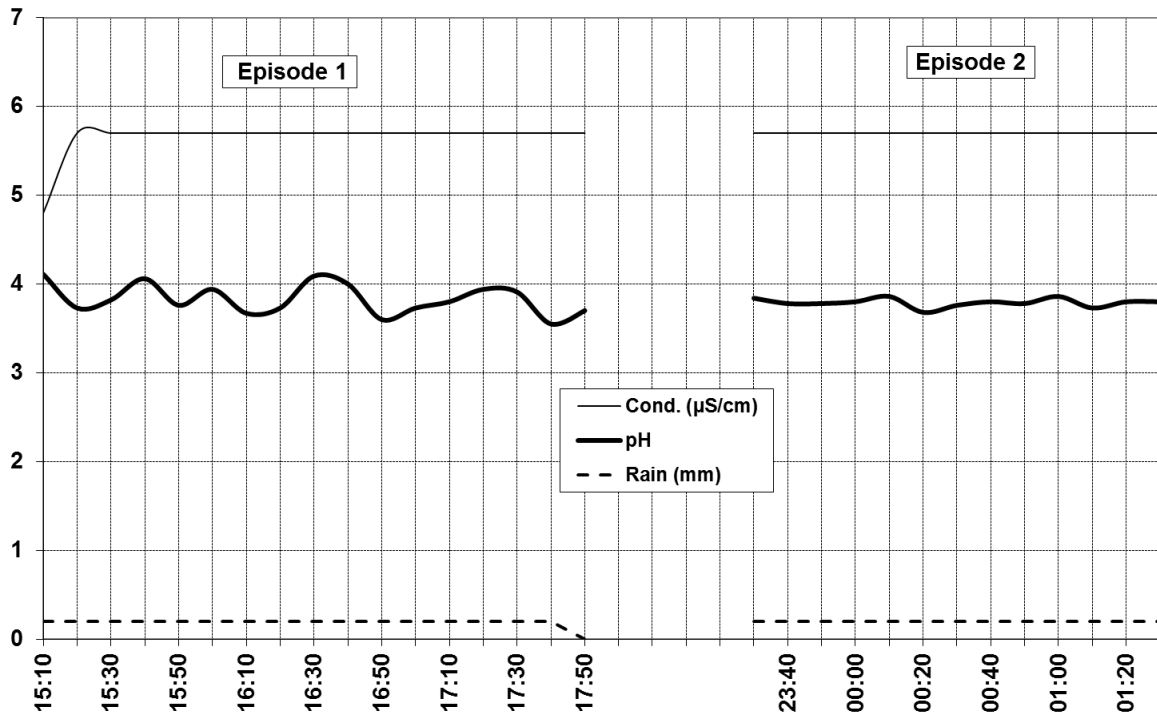


Figure 15: Records of pH and conductivity for the two rainfall episodes in the days 13th and 14th February 2008. The acidification of the rainfall shows intense values.

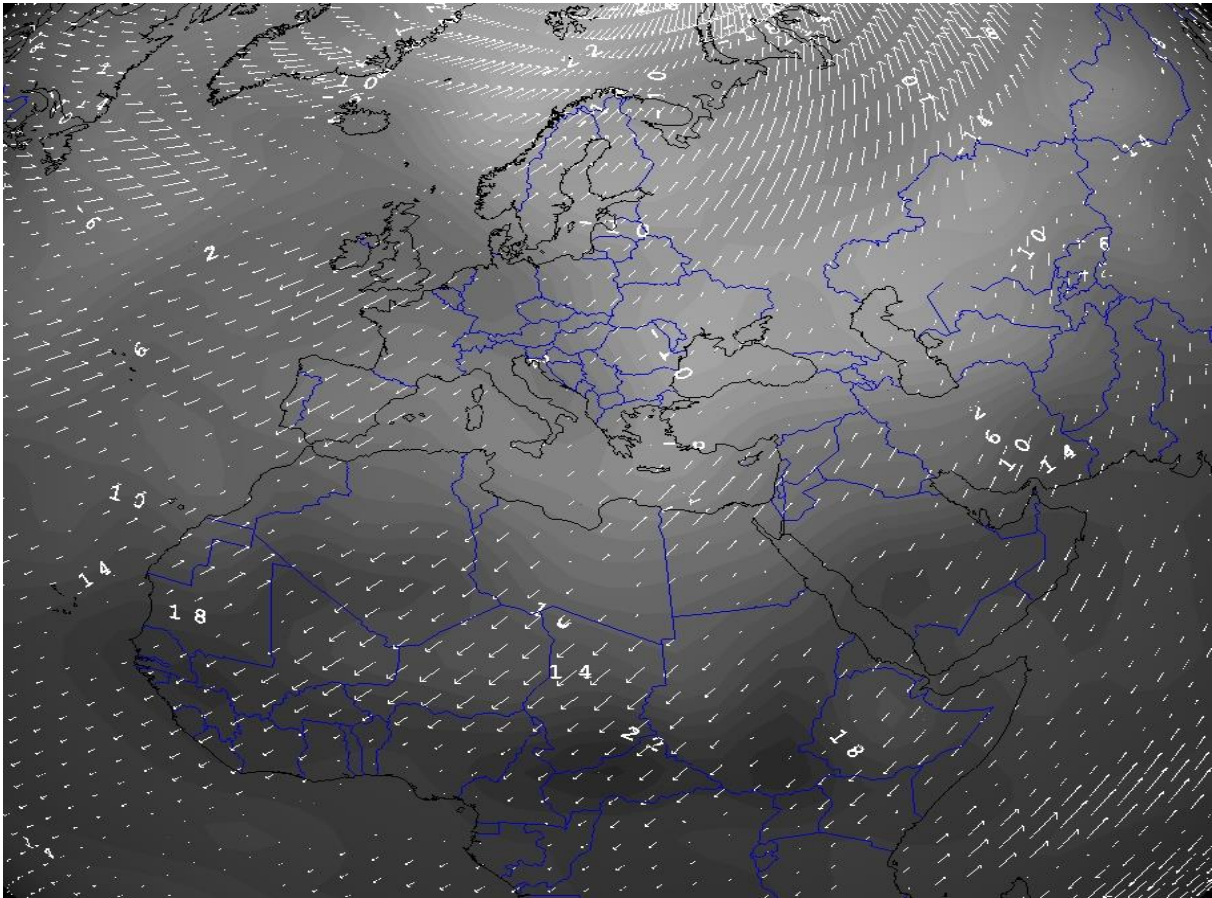


Figure 16: Air Temperature and flow vectors at 850 hPa level on February 14th, 2008 (NCEP Reanalysis data provided by the NOAA/OAR/ESRL PSD, Boulder, Colorado, USA, from their Web site at <http://www.esrl.noaa.gov/psd/>). Crisp cold air advection at 850 hPa height.

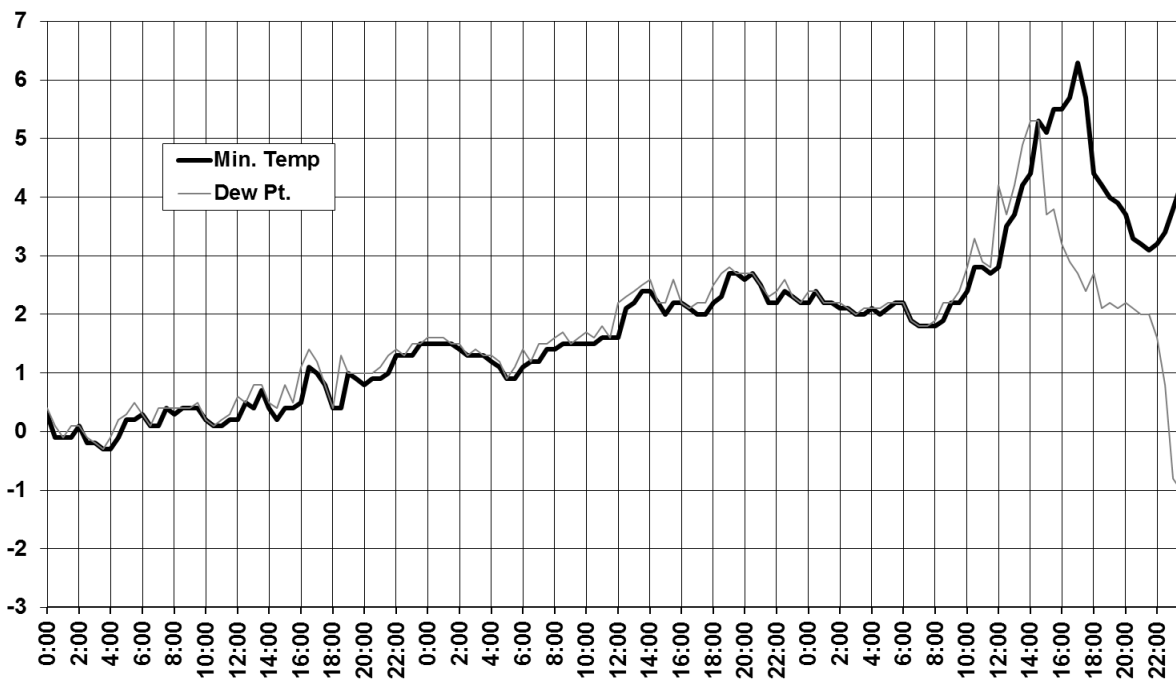


Figure 17: Thermal and dew point evolution (Td) in the University weather station of Fredes from the 13th to 15th February 2008.

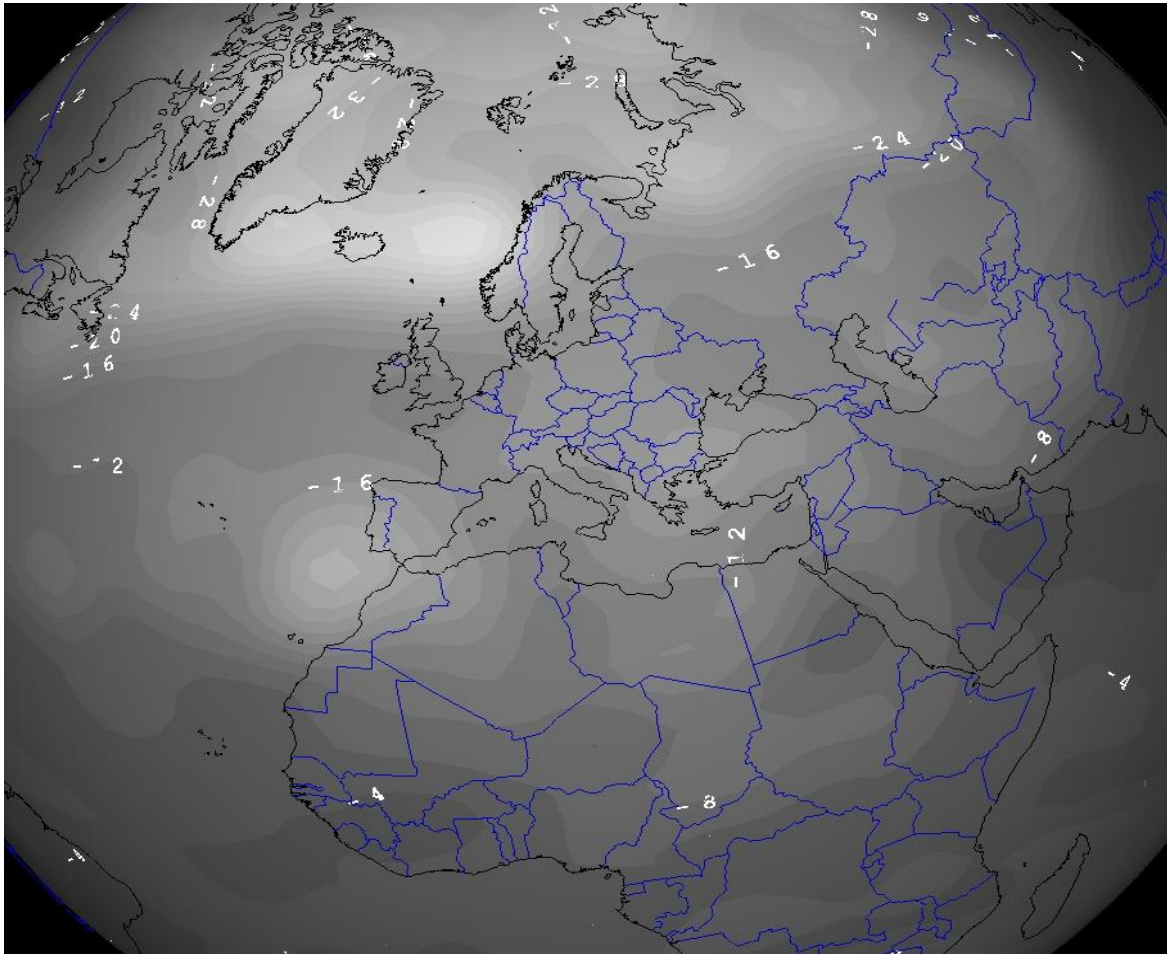


Figure 18: Air Temperature at 500 hPa level on May 23rd, 2007 (NCEP Reanalysis data provided by the NOAA/OAR/ESRL PSD, Boulder, Colorado, USA, from their Web site at <http://www.esrl.noaa.gov/psd/>). African aerosol on the western basin of the Mediterranean and cut-off low on the Gulf of Cadiz.

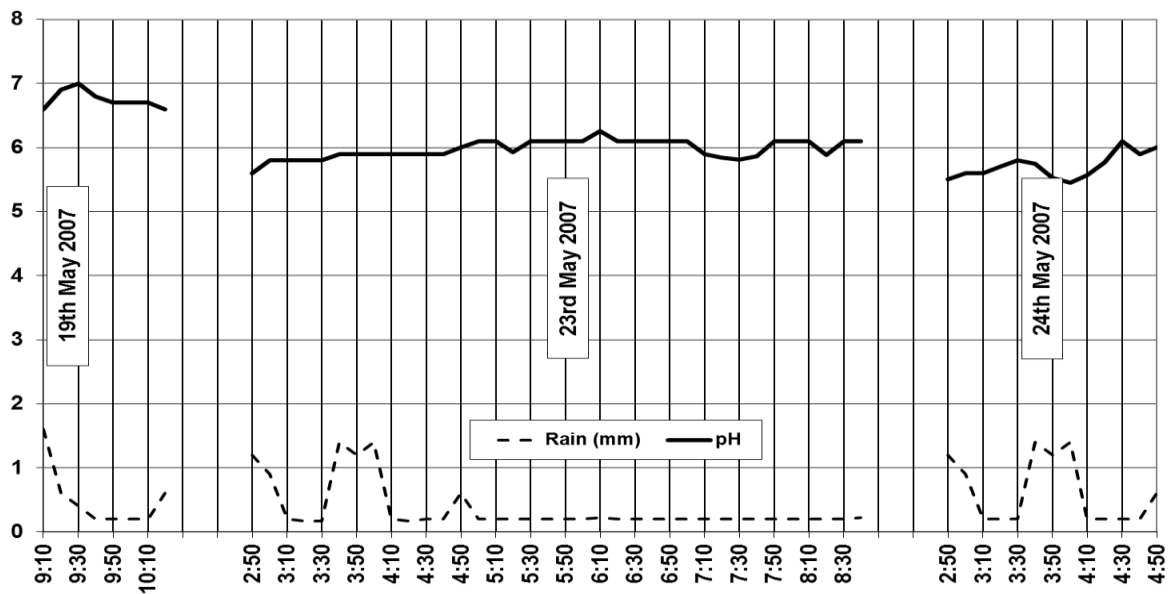


Figure 19: Analysis of rainwater precipitated in Torre Miró in 19th, 23rd and 24th May 2007.

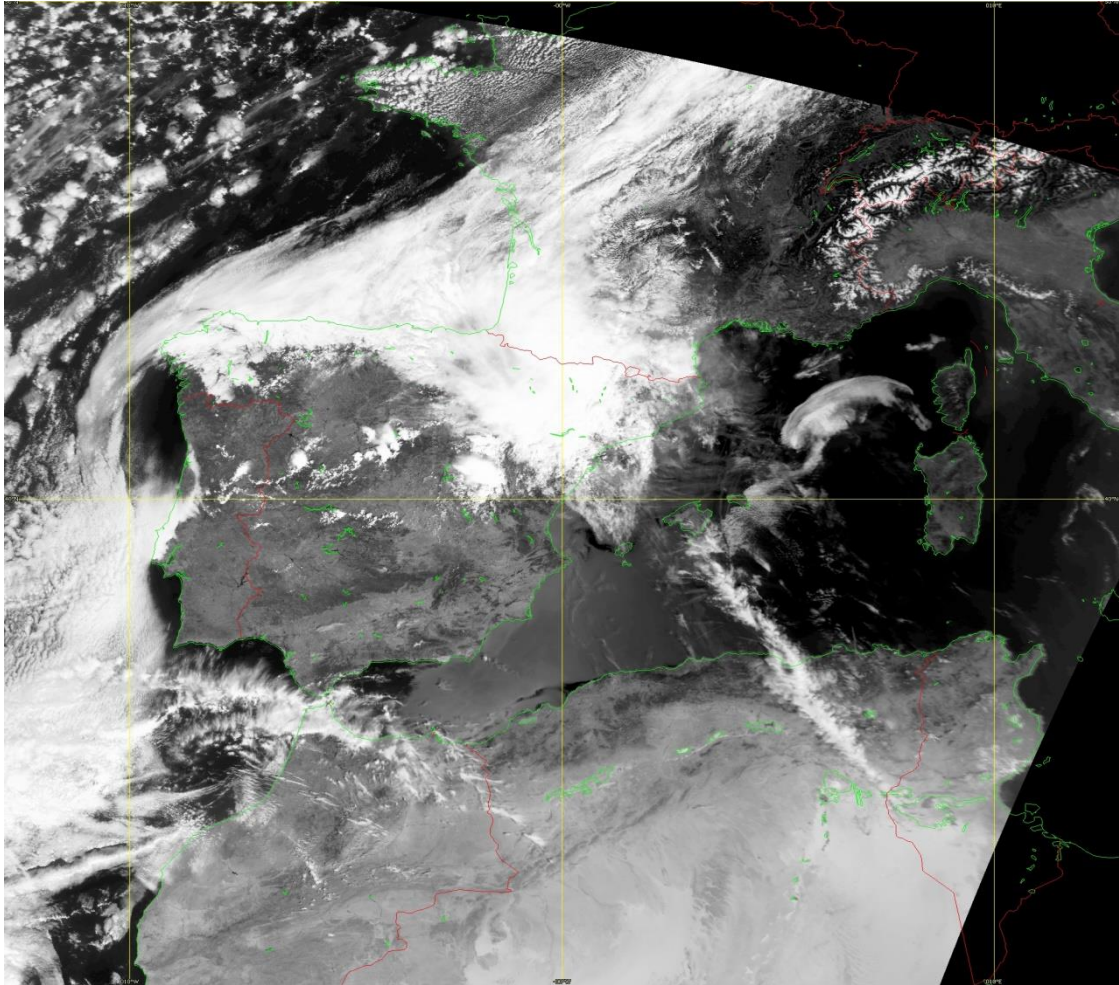


Figure 20: NOAA-AVHRR VIS image (Band 1, 0.580-0.680 μm Dartcom equipment), May 19th, 2007. The African aerosol overflows onto the Spanish Mediterranean region through the Alboran Sea. Dartcom HRPT Ground Station, Climate Laboratory, University Jaume I.

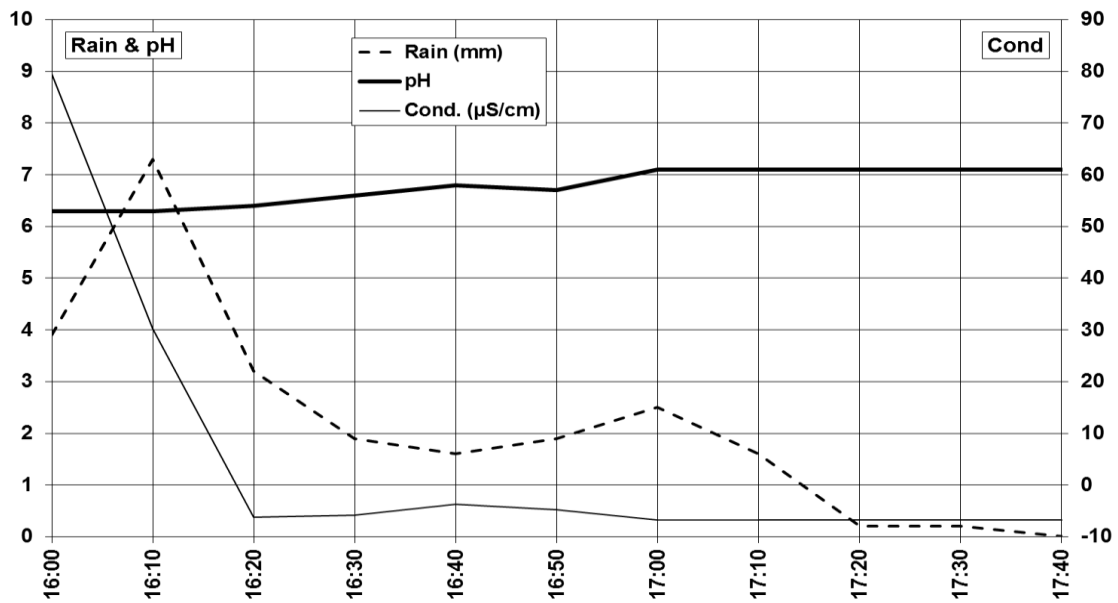


Figure 21: pH records on August 28th, 2012. The basic rain values are due to the neutralization of the African aerosol.

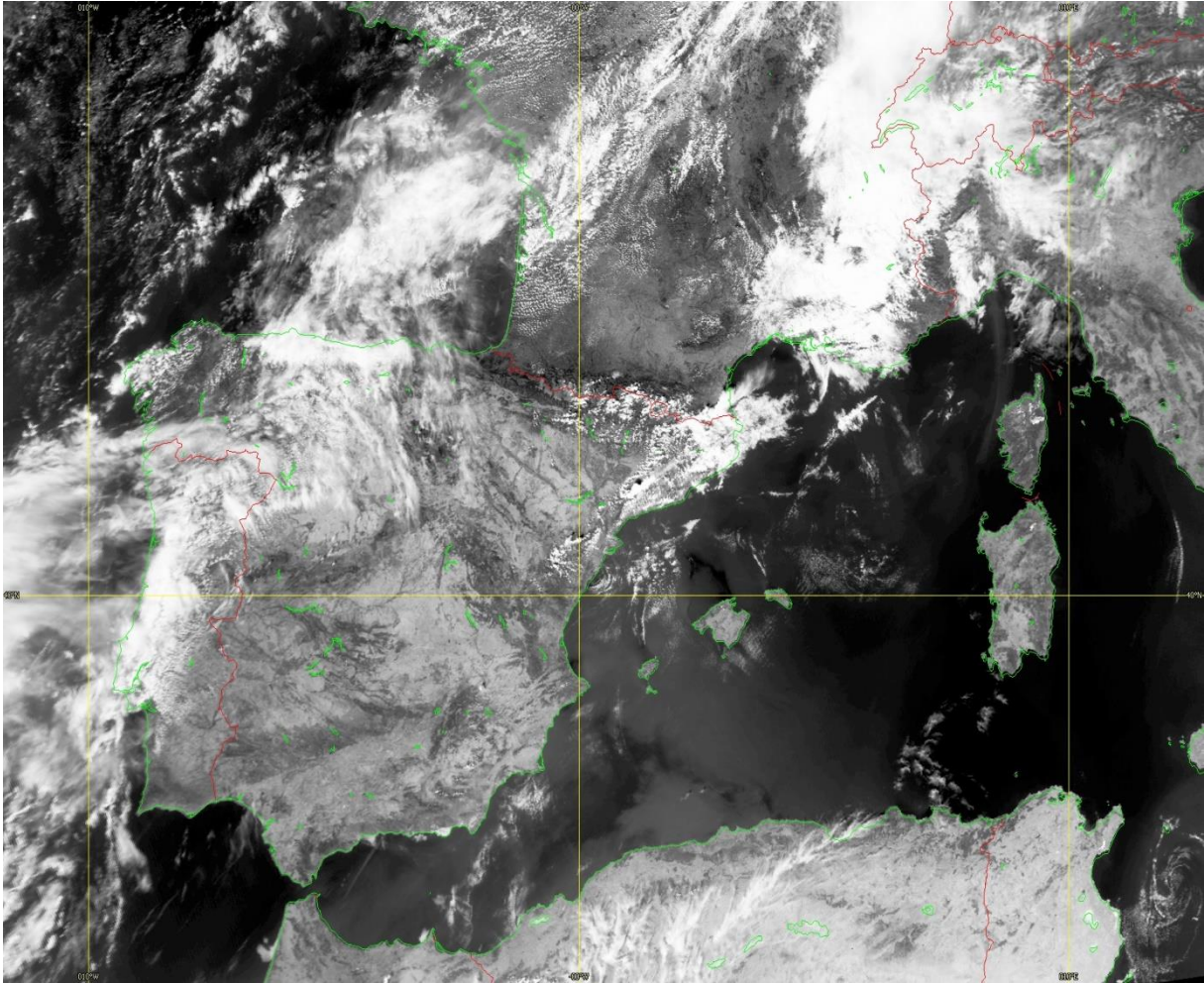


Figure 22: NOAA-AVHRR VIS image (Band 1, 0.580-0.680 μm Dartcom equipment), August 28th, 2012. The African aerosol flows over the Spanish Mediterranean region through the Alboran Sea. Dartcom HRPT Ground Station, Climate Laboratory, University Jaume I.